Longitudinal and Transverse Feedback Systems for BESSY-II

S. Khan and T. Knuth

BESSY-II, Rudower Chaussee 5, 12489 Berlin, Germany

Abstract. The commissioning of the high-brilliance synchrotron light source BESSY-II in Berlin started in April 1998. Within the commissioning period, bunch-by-bunch feedback systems to counteract longitudinal and transverse multibunch instabilities will be installed. This paper reviews their design and present status.

INTRODUCTION

BESSY-II [1] is a high-brilliance synchrotron radiation source currently being commissioned in Berlin. The first beam was stored on April 22, 1998.

The performance of a "third generation" light source can be seriously impaired by longitudinal and transverse multibunch instabilities leading to

- Limitations of the beam current,
- Increased beam spot and divergence due to transverse oscillations, and
- Broadening of the undulator line-width due to energy oscillations.

Multibunch instabilities are excited by long-range wakefields due to higher-order modes (HOMs) of the rf cavities or due to the finite wall conductivity. Presently, the BESSY-II storage ring will be operated with four DORIS-type pillbox cavities with a rich HOM spectrum. It is important to have control over the HOM position either by controlling the cavity temperature [2] or by adding a second plunger to the cavities. Both methods are currently under investigation. However, even in the most favorable case, radiation damping will not be sufficient to damp longitudinal instabilities at beam currents of several hundred mA. HOMs may also excite transverse instabilities under unfavorable conditions. However, the main source of vertical oscillations will be the resistive wall impedance, once insertion device chambers with small vertical apertures (± 8 mm and ± 5.5 mm, made of aluminum) are installed.

This paper describes the design and status of a longitudinal and a transverse bunch-by-bunch feedback system presently under construction.

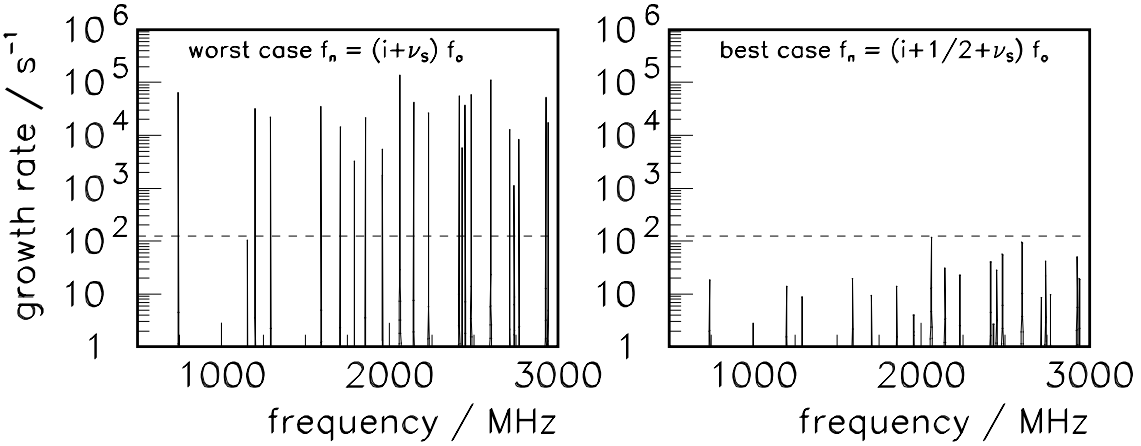

FIGURE 1. Longitudinal multibunch instability growth rates from HOMs at their most (left) and least (right) harmful position. The dashed line indicates the radiation damping rate.

LONGITUDINAL FEEDBACK SYSTEM

Longitudinal Multibunch Instabilities

Given the longitudinal shunt impedance $R_{\|n}$ of the n^{th} HOM, the central frequency f_n, and quality factor Q_n, the impedance as function of frequency f is given by

$$Z_{\|n}(f) = \frac{R_{\|n}}{1 + iQ_n\left(\frac{f}{f_n} - \frac{f_n}{f}\right)} \tag{1}$$

and the growth rate of a longitudinal multibunch mode m is given by

$$\frac{1}{\tau} = \frac{I\,\alpha}{2\nu_s E/e} \cdot \mathrm{Re}\sum_p f_p e^{-(2\pi f_p \sigma_t)^2} Z_{\|n}, \quad \text{with} \quad f_p = f_\circ(p\,h + m + \nu_s). \tag{2}$$

Here, I is the beam current, α is the momentum compaction factor, ν_s is the synchrotron tune, E/e is the beam energy, σ_t is the bunch length in time, $f_\circ$ is the revolution frequency, h is the harmonic number, and the impedance is sampled at all integer values of p.

The growth rates from HOMs predicted by a 2D MAFIA simulation in the frequency domain [3] are shown in Figure 1 for a beam current of 400 mA, considering two limiting cases:

- The "worst case," where the HOMs coincide with multibunch modes, and
- The "best case," with the HOMs between two multibunch modes.

Measurements indicate that the simulation tends to overestimate the shunt impedance and Q-value of HOMs [4], [5]. Using a network analyzer, the HOM

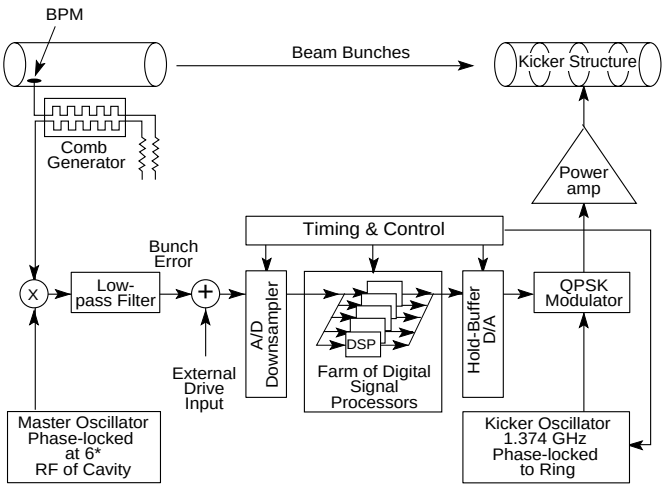

FIGURE 2. Block diagram of the longitudinal feedback system (courtesy SLAC LFB group).

frequencies and Q-values can be measured directly. Measuring the HOM frequency shift as function of the position of a small object in its field allows to identify the mode, while the integrated frequency shift measures the R/Q ratio. Measurements on a spare cavity are underway and first results indicate that the Q-values are indeed two to three times lower than predicted.

Longitudinal Feedback System Overview

The longitudinal system employs the digital electronics developed for ALS, PEP-II and DAΦNE [6]. Being developed and well tested over many years at the ALS, the advantages of this option for BESSY-II are minimum development effort, reliability, and well-maintained hardware and software. Furthermore, the digital system offers flexibility in the feedback algorithm and excellent diagnostic capabilities [7].

The block diagram in Figure 2 outlines the system. The bunch signal from a beam position monitor is fed into a comb generator to produce a 3-GHz signal for phase detection. The moment signal (phase·charge) is digitized at a rate of 500 MHz, downsampled and distributed to an array of DSPs, where a correction signal is computed for every bunch. The D/A-converted correction signal QPSK-modulates a carrier at 1374 MHz (11/4 times the rf frequency). More detailed descriptions of the electronics and the feedback algorithm can be found in [6], [8], [9], and [10].

Longitudinal Kicker Cavity

For the longitudinal kicker structure, a choice had to be made between a series of coaxial electrodes as used for the ALS and PEP-II [11] and a cavity-type kicker as developed for DAΦNE [12]. With only little space being available, the DAΦNE design, offering a larger shunt impedance in a single structure, was favored. For

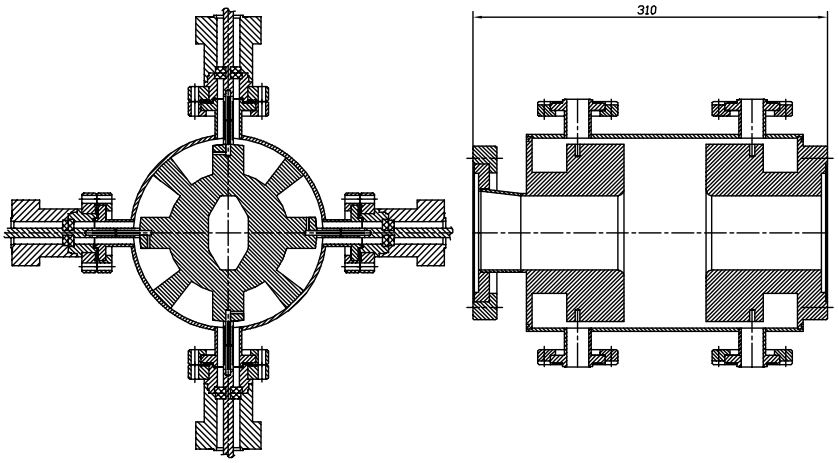

FIGURE 3. Strongly damped pillbox-type kicker cavity with eight waveguides.

BESSY-II, the kicker design required several modifications. The central frequency was moved from 1197 MHz to 1374 MHz, and the bandwidth was increased by using eight waveguides instead of six. Modifying the beam ports according to the BESSY-II chamber also increased the shunt impedance. Figure 3 shows the 31 cm long structure with a shunt impedance of $R_s \approx 1000\ \Omega$ and a Q-value of 5.6.

Longitudinal Damping Rates

The damping rate of the longitudinal feedback system can be expressed as

$$\frac{1}{\tau} = \frac{f_\circ\, h\, \alpha}{2\,\nu_s\, E/e} \cdot G, \tag{3}$$

with $G = \Delta U/\Delta\phi$ being the feedback gain, i.e., the kick voltage per unit phase deviation (radian), and all other symbols defined as before. The gain cannot be arbitrarily large, because the voltage is limited to $\Delta U \leq \sqrt{2NR_sP}$ for a total power P and N kickers. $\Delta\phi$ is limited by the phase resolution and beam noise.

Assuming a 250-W amplifier, one kicker, and 50% power loss, the maximum voltage is 500 V. As shown in Figure 4, saturation at $\Delta\phi = 7$ mrad leads to a maximum damping rate of 1000 s^{-1}. The maximum effective impedance $Z_{\parallel}^{\mathrm{eff}} = G/I$ is 180 kΩ. If necessary, performance can be improved by adding power, by using more kickers, or — subject to operational experience — by increasing the gain.

TRANSVERSE FEEDBACK SYSTEM

Transverse Multibunch Instabilities

The impedance of a given HOM and the resistive wall impedance is

$$Z_{\perp n}(f) = \frac{2\pi\, f_n^2}{c\, f} \cdot \frac{R_{\perp n}}{1 + iQ_n\left(\frac{f}{f_n} - \frac{f_n}{f}\right)} \quad \text{and} \quad Z_\perp^{\mathrm{rw}}(f) = \frac{c^2}{2\pi\, f_\circ\, f} \cdot \frac{1 - \mathrm{sgn}(f)\, i}{\pi\, b^3 \delta\, \sigma}, \tag{4}$$

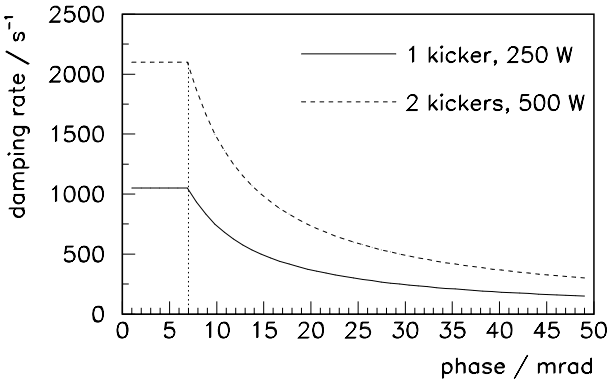

FIGURE 4. Longitudinal feedback damping rate as function of phase deviation.

where b is the half-aperture, $\delta \sim f^{-1/2}$ is the skin depth, and σ is the wall conductivity. The growth rate of rigid bunch transverse oscillations is

$$\frac{1}{\tau} = \frac{I\,c^2}{4\pi\,\nu f_\circ\,E/e}\mathrm{Re}\sum_p e^{-(2\pi\sigma_t)^2(f_p-\frac{\xi}{\alpha}f_\circ)^2}\,Z_\perp(f_p) \quad \text{with} \quad f_p = f_\circ(p\,h+m+\nu), \quad (5)$$

where ν is the betatron tune, ξ is the chromaticity, and all other symbols are defined as before. Figure 5 shows the resistive wall growth rate as function of betatron tune and chromaticity.

Transverse HOMs can be obtained from a 3D MAFIA simulation, taking into account the three ports of the DORIS cavity that break the rotational symmetry. In a picture analogous to Figure 1, the "worst case" growth rates for some modes can reach 10^4 s^{-1}.

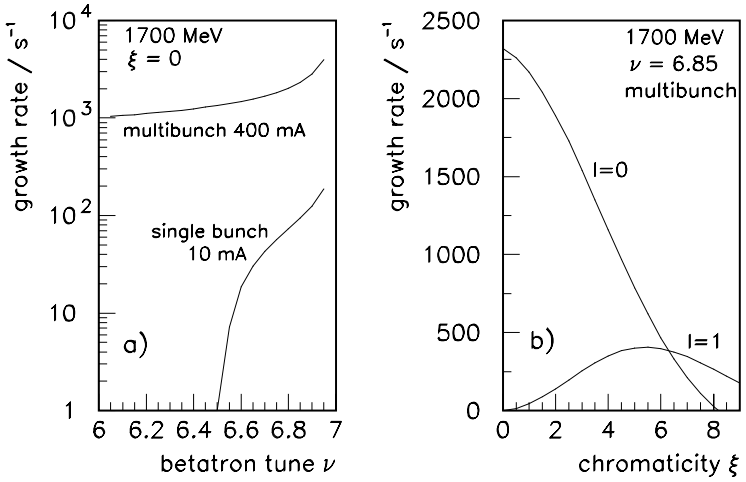

FIGURE 5. Resistive wall effect: growth rate as function of betatron tune and chromaticity.

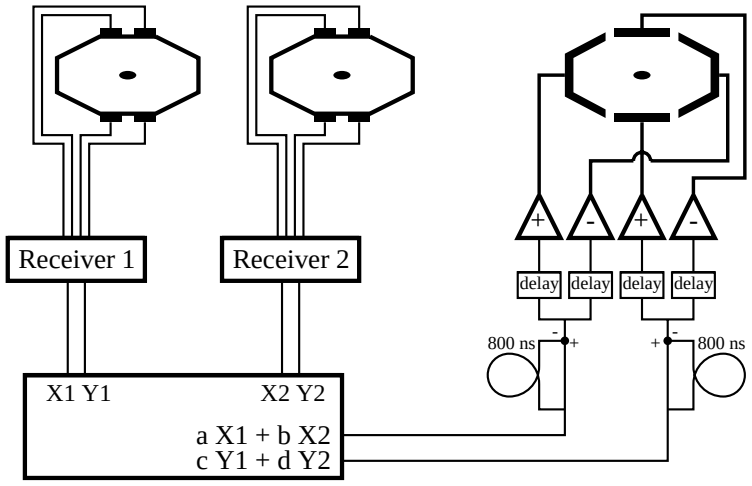

FIGURE 6. Block diagram of the transverse feedback system.

Transverse Feedback System Overview

For BESSY-II, the transverse feedback system will be modeled after the analog system developed for the ALS [13], [14]. Figure 6 shows a block diagram of the system, where signals from two sets of button-type pickups approximately 90° apart in betatron phase are used. The moment signals (displacement·charge) are detected at 3 GHz, differenced, mixed down to baseband, and combined in proper proportion. For offset rejection, the correction signals from subsequent revolutions are subtracted. The resulting kicks are provided by stripline kickers, where either one or — as shown in the figure — both electrodes are driven by a power amplifier.

Transverse Stripline Kicker

The transverse stripline kicker combines horizontal and vertical electrodes in one structure, which minimizes space requirements and leads to a low loss factor. The electrodes are shaped according to the octagonal vacuum chamber. Despite some coupling between horizontal and vertical electrodes, the small distance of the electrodes to the beam (32 mm and 17.5 mm) leads to a sufficiently large vertical kicker shunt impedance of 20 kΩ at low frequency, dropping to 10 kΩ at 250 MHz. In the horizontal coordinate, where no resistive wall effect is anticipated, the shunt impedance is lower by a factor of 2. The electrodes have a line impedance of 50 Ω and are 30 cm long, to minimize power picked up from the 500 MHz bunch sequence. A simplified MAFIA model of the kicker for wakefield and 3D electrostatic computation is shown in Figure 7.

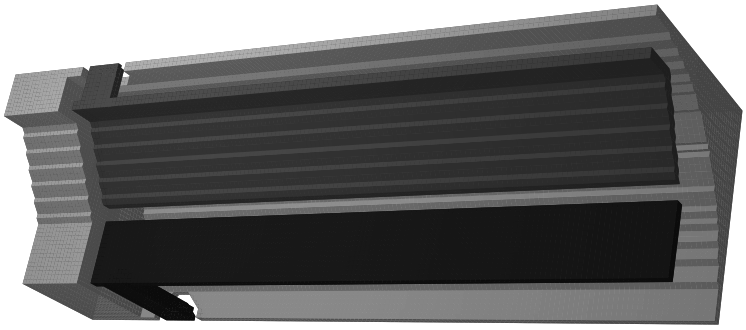

FIGURE 7. MAFIA model of the transverse feedback kicker (1/8 of the full structure).

Transverse Damping Rates

The damping rate of the transverse feedback system is given by

$$\frac{1}{\tau} = \frac{f_\circ \sqrt{\beta_1 \, \beta_2}}{2\,E/e} \cdot G, \tag{6}$$

where β_1 and β_2 are the beta functions at the pickup and at the kicker position, respectively, and $G = \Delta U/\Delta y$ is the gain, i.e., the kick voltage per unit displacement.

With a 100 W amplifier connected to each vertical electrode and assuming 50% power loss, the maximum voltage at low frequency is 2000 V. For saturation at $\Delta y = 1$ mm, the maximum damping rate is 4400 s^{-1}, dropping to 3100 s^{-1} at 250 MHz, as shown in Figure 8. The maximum impedance $Z_\perp = G/I$, that can be counteracted at a beam current of 400 mA, is 5 MΩ, whereas the resistive wall impedance is estimated to be 2 MΩ at the lowest frequency.

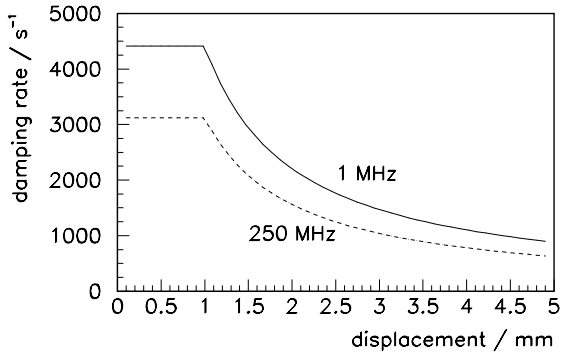

FIGURE 8. Transverse feedback damping rate as function of transverse displacement.

SUMMARY AND PRESENT STATUS

The design effort for feedback systems to counteract multibunch instabilities has been minimized by making use of the developments and experience that other facilities (SLAC, ALS, DAΦNE) have generously made available to BESSY.

The longitudinal feedback electronics have been fabricated and most of the commercially available components have been ordered. For the transverse feedback system, the components for the mixer and one receiver have been purchased and a prototype will be built during summer 1998. For both systems, existing button-type pickups can be used. The kickers for both systems will be installed in a straight section used for diagnostic purposes. First beam test opportunities will occur in several machine study periods toward the end of 1998.

ACKNOWLEDGMENTS

The help of W. Barry, J. Byrd, J. Corlett, and G. Stover (ALS, Berkeley); of J. Fox, H. Hindi, S. Prabhakar, and D. Teytelman (SLAC, Stanford); and of A. Gallo, F. Marcellini, M. Serio, and M. Zobov (INFN, Frascati) is gratefully acknowledged.

This work is funded by the Bundesministerium für Bildung, Wissenschaft, Forschung und Technologie and by the Land Berlin.

REFERENCES

1. Jaeschke, E., *Proc. of the 1997 Part. Acc. Conf., Vancouver*, in print (1997).
2. Svandrlik, M., et.al., *Proc. of the 1995 Part. Acc. Conf., Dallas*, 2762 (1995).
3. MAFIA Collaboration, *MAFIA Manual*, CST GmbH, Darmstadt (1996).
4. Corlett, J. N. and J. M. Byrd, *Proc. of the 1993 Part. Acc. Conf., Washington DC*, 3408 (1993).
5. Bartalucci, S., et al., *Part. Acc.* **48**, 213 (1995).
6. Teytelman, D., et al., *Proc. of the 1995 Part. Acc. Conf., Dallas*, 2420 (1995).
7. Prabhakar, S., et al., *Part. Acc.* **57**, 175 (1997).
8. Teytelman, D., et al., SLAC-PUB-7305 (1996).
9. Hindi, H., S. Prabhakar, J. Fox, and D. Teytelman, *Proc. of the 1997 Part. Acc. Conf., Vancouver*, in print (1997).
10. Young, A., J. Fox, and D. Teytelman, *Proc. of the 1997 Part. Acc. Conf., Vancouver*, in print (1997).
11. Corlett, J. N., et al., *Proc. of the 1994 Europ. Part. Acc. Conf., London*, 1625 (1994).
12. Boni, R., et al., *Part. Acc.* **52**, 95 (1996).
13. Barry, W., et al., *Proc. of the 1993 Part. Acc. Conf., Washington* 2109 (1993).
14. Barry, W., et al., *Proc. of the 1994 Europ. Part. Acc. Conf., London*, 122 (1994).